# Spectral diffusion in liquids

Alan D. Stein[a] and M. D. Fayer
*Department of Chemistry, Stanford University, Stanford, California 94305*

(Received 1 April 1992; accepted 22 May 1992)

Spectral diffusion of an electronic transition of solute chromophores in liquid solutions is investigated experimentally and theoretically through its influence on electronic excited-state transfer (EET). Observation of dispersive EET in liquids (the EET rate depends on the excitation wavelength) demonstrates that absorption lines are inhomogeneously broadened on a nanosecond time scale in the systems studied although the time scale for homogeneous dephasing is tens of femtoseconds. A theory is developed that relates the rate of spectral diffusion to the wavelength dependence and temperature dependence of EET. Time-resolved fluorescence depolarization measurements are used to measure EET in the systems rhodamine B (RB) in glycerol and propylene glycol as a function of wavelength and temperature from room temperature (298 K) to 200 K. Comparison with theory permits the rates of the solvent fluctuations responsible for spectral diffusion to be determined for the two solvents at several temperatures. Measurements are also made of the rates of solvent relaxation about the excited RB and of RB orientational relaxation. The results demonstrate that the mechanism for spectral diffusion is solvent orientational relaxation which causes the initial (time of optical excitation) dipolar field, produced by the solvent at the chromophore, to randomize.

## I. INTRODUCTION

Molecular liquids undergo extremely complex dynamic behavior; both solutes and solvents undergo a variety of processes, e.g., translation, rotation, libration, each of which occurs on a characteristic time scale. Solutes experience the dynamics of the bulk medium via intermolecular interactions that couple internal and external degrees of freedom. These time-dependent intermolecular interactions give rise to dynamically broadened optical-absorption spectra. While it is clear that the dynamics of the medium produce broadened spectra, it is a complex problem to work backwards from a spectrum to the dynamics of a particular system. Recent advances in theory[1] and optical experiments[2] are beginning to make it possible to examine liquid dynamics using line shapes (optical dephasing in the time domain) obtained from optical line-narrowing experiments.

Electronic excitation transfer (EET) among aromatic molecules has been studied extensively.[3–18] In this paper we report the first detailed study of the influence of multi-time-scale dynamics of liquids on solute molecules. The dynamics are revealed by the influence of spectral diffusion on EET observables. The basis for this investigation was established by recent experimental and theoretical advances in the use of optical line-narrowing experiments to study dynamics in complex systems, particularly low-temperature glasses.[19] Dynamical processes in complex media can occur over a broad distribution of time scales (broad fluctuation rate distribution). For example, at 1.5 K, ethanol glass undergoes structural fluctuations that span time scales from picoseconds to thousands of seconds.[20] The bath fluctuations couple to the optical transition of a dissolved chromophore and cause dephasing (line broadening) over this range of time scales.

Dynamic broadening results from fluctuations in solvent–solute interactions that perturb the electronic states of the chromophore on the same time scale or faster than a particular spectroscopic measurement. Dynamic line broadening encompasses both homogeneous dephasing and broadening that results from spectral diffusion.[19(a)] The distinction between homogeneous dephasing and spectral diffusion is significant, although it is actually a question of time scales. Optical measurements can reflect the combined effects of homogeneous dephasing and spectral diffusion if the measurement has the appropriate characteristic time scale.[19,20]

A number of techniques have been developed to measure dynamic line broadening.[19(a),21,22] Photon-echo experiments[23,24] measure the homogeneous dephasing time of a chromophore. Optical hole burning and fluorescence line narrowing[22,25] reflect contributions to dynamic broadening from homogeneous dephasing as well as spectral diffusion. The hole-burning measurements made on chromophores in low-temperature glasses have clearly demonstrated that the amount of dynamic line broadening observed using a particular method depends on the characteristic time scale associated with the measurement.[19,26]

Recently, measurements of photon echoes and hole burning have been made on liquids at room temperature.[27] Femtosecond time-scale photon-echo experiments have shown that electronic dephasing times are on the order of 60 fs in viscous hydrogen-bonding liquid solutions at room temperature.[2] Transient hole-burning measurements indicate that inhomogeneous broadening can be observed in liquids for times as long as several picoseconds at room temperature.[27–29]

[a]Permanent address: Rohm & Haas Co., Research Laboratories, Bristol, PA 19007.

 0021-9606/92/172948-15$006.00 

In what follows, we will present theory and experiments that permit quantitative information to be obtained on the rate of spectral diffusion in liquids. To discuss this it is necessary to briefly describe the relationship between observables and the fluctuation rates in liquids. Results that have emerged from the optical line-narrowing research on low-temperature glasses are relevent to room-temperature liquids. All optical line-narrowing experiments that have been performed to date can be described in terms of a four-time correlation function.[19(b),30,31] While there are differences in the details, all of the four-time correlation functions can be obtained from the four-time correlation function that describes the stimulated photon-echo experiment.[31] For example, it has been demonstrated that an optical hole-burning experiment is described in terms of the Fourier transform of the stimulated echo correlation function. A hole-burning experiment is a frequency-domain stimulated echo experiment. In magnetic resonance, the stimulated echo is a standard experiment used to measure spectral diffusion. There are two distinct times in the experiment, $\tau$ and $T_w$. $\tau$ is on the order of the homogeneous dephasing time. Fast fluctuations on the time scale $\tau$ or faster contribute to homogeneous dephasing. $T_w$ is generally a longer time. Slow dynamics out to the time scale $T_w$ can contribute to line broadening (dephasing). This contribution to the dynamic linewidth is referred to as spectral diffusion.

Because the description of frequency-domain experiments, such as hole burning and fluorescence line narrowing, is related to the Fourier transform of the stimulated echo correlation function, it is not surprising that these experiments are sensitive to spectral diffusion. A photon-echo experiment is the limit of a stimulated echo experiment with $T_w$ equal to zero. Therefore, the photon echo measures the homogeneous dephasing only.

Recent photon-echo experiments on dye molecules in hydrogen-bonding liquids, which have measured a 60 fs dephasing time, demonstrate that homogeneous dephasing results from very fast fluctuations in a room-temperature liquid.[2] However, as discussed above, the photon echo is not sensitive to the slower time-scale fluctuations that would result in additional line broadening by spectral diffusion. In fact, the very observation of a photon echo demonstrates that on the echo time scale, the system is inhomogeneously broadened. In a liquid, on some accessible time scale, a solute chromophore will experience all possible solvent configurations. On a long enough time scale, the optical line will be completely dynamically broadened by spectral diffusion. Thus the photon-echo experiments and very fast hole-burning experiments in liquids may provide only partial information on liquid dynamics that contribute to optical line broadening. These experiments will not be sensitive to much slower dynamics that ultimately dynamically broaden the entire line, eliminating inhomogeneous broadening.

The observation of dispersive EET by time-resolved fluorescence depolarization[32,33] is closely related to optical line-narrowing experiments. EET experiments, as presented below, with associated theory, can be used to obtain information on the rate and mechanism of slow time-scale (ns) spectral diffusion in liquids.

In a time-resolved fluorescence depolarization EET measurement, a small number of chromophores are excited with a short pulse of polarized light. Once an excitation is produced, it can jump to an unexcited chromophore (EET). If fluorescence occurs prior to EET, the emission is polarized. However, EET takes the excitation into the randomly oriented ensemble of initially unexcited chromophores. Subsequent emission is depolarized. Therefore, the rate of fluorescence depolarization is directly related to the rate of EET.[5,4,16]

Förster demonstrated that the rate of EET is related to the spectral overlap of the emission spectrum of the initially excited molecule (donor) and the absorption spectrum of the molecule that receives the excitation (acceptor). The acceptor may be chemically identical to the donor. Förster assumed homogeneously broadened spectra. For identical molecules, the forward transfer rate is the same as the back transfer rate; the rate depends on the inverse sixth power of the distance between the molecules. If the spectra are inhomogeneously broadened, the forward and back transfer rates may differ even for identical molecules. If a donor transfers to an acceptor with much lower energy (red side of the spectrum), the thermal energy may not be sufficient to permit back transfer. In this case, EET moves the excitation to lower energy as well as spatially. This is termed dispersive transport. Dispersive EET has been addressed both experimentally and theoretically.[32–40] The amount of dispersive character depends on the relative contributions of dynamic and inhomogeneous broadening to the electronic transition.

The influence of spectral linewidths on the rate of EET causes the transfer event to carry information on the linewidths to the fluorescence polarization observable. The excitation transfer time is analogous to $T_w$ in a line-narrowing experiment. In a system undergoing excitation transport and spectral diffusion on the same time scale, the rate and the excitation wavelength dependence of the fluorescence depolarization reflect the time dependence of the spectral diffusion.

If spectral diffusion is fast compared to EET, the lines are dynamically broadened on the EET time scale. This is the Förster limit. Transport is nondispersive, and the fluorescence depolarization observable is independent of the excitation wavelength. If spectral diffusion is slow compared to EET, the line is inhomogeneously broadened on the EET time scale. This is analogous to recent dispersive transport experiments in polymeric glasses at room temperature.[32] Characteristic wavelength and temperature dependences are observed. When spectral diffusion is on the time scale of EET, the EET dynamics, and therefore the fluorescence depolarization observable, are strongly influenced by spectral diffusion. The characteristics of the transfer can change during the course of the excited-state lifetime, from highly dispersive at short time to nondispersive at long time.

In this work, spectral diffusion is introduced into the model of dispersive transfer that was developed to describe

EET in polymer glasses.[32] A recent theoretical result is employed that relates the time dependence of the spectral diffusion contribution to the dynamic linewidth of the chromophore to the rate distribution of dynamics occurring in the solvent.[19(b)]

We also present dispersive EET experiments on liquids at temperatures well above $T_g$.[33] Measurements have been made at and near room temperature on solutions of rhodamine B in glycerol and propylene glycol, two hydrogen-bonding solvents that have glass transition temperatures below 200 K. The EET is dispersive in glycerol at room temperature and below, and in propylene glycol at 273 K and below. By examining the wavelength dependence of the dispersive EET in the two liquids at several temperatures, we are able to determine the rate of the underlying process responsible for spectral diffusion. The results demonstrate that molecular reorientation of the solvent molecules is responsible for spectral diffusion. Rhodamine B undergoes a large change in dipole moment upon excitation. The molecular dipole couples to the solvent dipoles. For fixed solvent configuration, the solvent is responsible for a dipolar field at the chromophore. This determines the chromophore's initial position in the inhomogeneous absorption spectrum. As the solvent structure evolves through orientational relaxation, the dipolar field at the chromophore changes, resulting in spectral diffusion. This time scale is 5 orders of magnitude longer than the tens of femtoseconds electronic dephasing time scale measured in recent photon-echo experiments. The solvent dynamics leading to spectral diffusion on a nanosecond time scale are fundamentally different from the interactions that cause homogeneous dephasing of electronic states.

## II. THEORY

Recently, a model was developed to describe dispersive excitation transfer among chromophores in solid solutions at and near room temperature.[32] It was assumed that the magnitude of dynamic line broadening (assumed to be homogeneous broadening) and the extent of inhomogeneous broadening were time independent, i.e., it was assumed that spectral diffusion does not occur on the time scale over which excitation transfer takes place. This is a reasonable assumption for solids. Calculations of the time dependence of EET using this model without adjustable parameters were in near quantitative agreement with experimental measurements made on polymeric systems at and below room temperature. This range of temperatures is well below the polymer glass transition temperature. The model provided the essential features of dispersive transfer from a mathematically tractable calculation.

In this section we introduce spectral diffusion into the calculations of dispersive transport. This is done by allowing both the dynamic and inhomogeneous line shapes and linewidths to change with time. Calculations of excitation transfer using this model illustrate the connection between the time scale for evolution of solvent structures and the dynamics of dispersive transport. The quantity of interest is $G^s(t)$,[6] the self-part of the Green-function solution of the transport master equation. $G^s(t)$ can also be identified with the time-dependent probability that an initially excited chromophore is still excited, excluding lifetime decay. Calculation of this quantity allows direct comparison with experimental measurements of $G^s(t)$ obtained from time-dependent fluorescence depolarization.

### A. Spectral diffusion

Recently, Bai and Fayer presented a theoretical analysis of optical line-narrowing measurements in systems with broad solvent (bath) fluctuation rate distributions.[19(b)] They obtained expressions relating the time dependence of solute optical line broadening to the probability distribution of $R$, the rates of dynamical processes in the solvent. The formalism is based on a four-point correlation-function description of line-narrowing experiments. It has also been demonstrated experimentally that a change in the optical dephasing rate (dynamic linewidth) as a function of the time scale of the measurements contains detailed information about the fluctuation rate distribution (the probability distribution of the rates, $R$) in the system.[19(b),20,26(c),41] As discussed in the Introduction, the dispersive EET fluorescence depolarization experiment is analogous to the line-narrowing experiments described by Bai and Fayer.

An expression is obtained in Ref. 19(b) for the derivative of the dynamic linewidth ($\Delta\omega_d$) with respect to time,

$$\frac{d(\Delta\omega_d)}{dt} \propto \int du\, P_1(e^u)\, W(u-v), \tag{1}$$

where $u=\ln R$, $v=-\ln(t)$, $P_1(e^u)$ is the solvent fluctuation rate distribution, and $W(u-v)$ is a function that depends on the nature of the fluctuations of the bath. $W(u-v)$ is called the gate function. Equation (1) states that the change in the linewidth with the time scale of the measurement is proportional to the convolution of the fluctuation rate distribution and the gate function.

This gate function, although an intrinsic physical property, acts much like an instrument response function of, for example, a gated integrator. If the fluctuation rate distribution is very broad, the change in the dynamic linewidth with time depends only on the form of the rate distribution. For a very narrow distribution, e.g., a single rate (a $\delta$-function distribution), the change in linewidth tracks the gate function. Independent of the nature of the bath fluctuations, the gate function has two characteristics. For a single rate, $R$, it is peaked at the observation time $T_w = 1/R$, and it has a width on the order of $\ln(1/T_w)$. Thus the linewidth will begin to broaden for observation times significantly shorter than $1/R$ and it will continue to broaden out to observation times significantly longer than $1/R$.

The gate function has been derived for the case of dipole–dipole coupling between the chromophore and a bath (solvent) that is undergoing quasicontinuous motion that can be described as a Gaussian–Markoffian stochastic process.[19(b)] This is the relevant gate function for the experiments discussed below. The result is

$$W(z)=\exp(z-e^z)\,[1-\exp(-e^z)\,]^{1/2}. \tag{2}$$

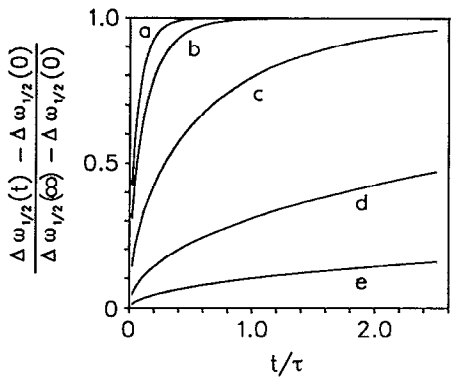


FIG. 1. Dynamic linewidth as a function of time for different values of the rate of solvent fluctuation ($R$). The curves are calculated using Eqs. (1) and (2). The dynamic width $[\Delta\omega_d(t)]$ is normalized by its value at $t=0$, the homogeneous width, and at $t=\infty$, when the spectral line is dynamically broadened. $R$ is parametrized in terms of fluorescence lifetimes: (a) $R=10$, (b) $R=5$, (c) $R=1$, (d) $R=0.1$, (e) $R=0.01$.

Use of Eq. (2) in Eq. (1) allows us to calculate the spectral diffusion contribution to the dynamic linewidth for a given solvent fluctuation rate distribution.

Ultrafast processes in liquids can give rise to homogeneous dephasing on a tens of femtosecond time scale.[2] If we adopt a model in which only one slow time-scale dynamic process with a single rate, $R$, causes spectral diffusion, then $P_1(R)$ in Eq. (1) is a $\delta$ function. Figure 1 shows the time-dependent dynamic linewidth calculated with Eqs. (1) and (2) for various values of the single-solvent fluctuation rate, $R$. $R$ is parametrized in chromophore excited-state lifetimes, $\tau$, i.e., $R=1$ means $R=1/\tau$. The two limits for the dynamic linewidth are the homogeneous linewidth (dynamic linewidth at $t=0$) which can be measured by a photon-echo experiment and the value at $t=\infty$, which is the width of the entire absorption origin since a chromophore in a liquid will eventually sample all solvent configurations and therefore all positions in the absorption band. In Fig. 1 the dynamic linewidth is plotted in terms of the fractional change in the linewidth:

$$[\Delta\omega_d(t)-\Delta\omega_d(0)]/[\Delta\omega_d(\infty)-\Delta\omega_d(0)].$$

For $R=10$ (Fig. 1, curve a), spectral diffusion broadens the line rapidly and the dynamic linewidth approaches its maximum value in a small fraction of a fluorescence lifetime. For $R=0.01$ (curve e), spectral diffusion causes only a small amount of broadening during the excited-state lifetime. For $R<0.01$, the inhomogeneous contribution to the line will be time independent on this time scale. EET, the observable in the measurements reported here, typically occurs on the time scale of the excited-state lifetime for weakly interacting chromophores. Thus, the latter case ($R<0.01$) is identical to the dispersive EET problem treated previously for frozen polymers.[32] For $R\gg 10$ the line will be completely dynamically broadened on the $\tau$ time scale; EET will not be dispersive, and Förster theory will be a valid description.

### B. Nondispersive transfer

Huber and co-workers employed a cumulant expansion to develop a mathematically tractable method for calculating $G^s(t)$ in the case of donor–donor transfer among randomly distributed chromophores.[9] The theory has more recently been extended to more complicated geometrical distributions.[10(b),11,12]

Donor–donor (DD) transfer occurs when the rate of forward energy transfer, transfer away from the initially excited chromophore to an acceptor chromophore, is equal to the rate of back transfer from the acceptor. In the Förster theory, identical molecules will undergo DD transfer. Donor–trap (DT) transfer occurs if the rate of back transfer is vanishingly small. Only forward transfer occurs from the donor to the trap. DT transfer takes place between two chromophores with electronic transition energies that differ by an amount greater than the available bath thermal energy. This can occur between two nonidentical molecules or identical molecules that are widely separated in a broad inhomogeneous line.

From the first-order cumulant expansion,

$$\ln G^s(t)=-\frac{\rho}{\lambda}\int (1-e^{-\lambda\omega(\mathbf{r})t})u(\mathbf{r})d\mathbf{r}, \tag{3}$$

$$\lambda=\begin{cases}1 & \text{for DT,}\\ 2 & \text{for DD.}\end{cases}$$

The two limits of EET differ by the value of the constant $\lambda$. $\omega(\mathbf{r})$ is the pairwise transfer rate for two chromophores separated by the three-dimensional vector $\mathbf{r}$. For a transition-dipole–transition-dipole interaction that is appropriate for singlet electronic states,

$$\omega(r)=(1/\tau)\cdot(R_0/r)^6\cdot\gamma^2. \tag{4}$$

$\tau$ is the excited-state lifetime and $R_0$ is the Förster transfer radius that depends on the spectral overlap between the emission spectrum of the donor and absorption spectrum of the acceptor.[17,42] $\gamma$ is a factor that accounts for orientational averaging of the donor and acceptor: $\gamma=1$ for the dynamic limit (reorientation occurs much faster than excitation transfer), and $\gamma=0.8452$ for the static limit (reorientation occurs at a much slower rate than transfer).[5,11] $u(\mathbf{r})$ is the chromophore spatial distribution function and $\rho$ is the number density of chromophores.

The analytical solution for a three-dimensional, randomly distributed solution of chromophores is[9,11]

$$\ln G^s(t)=-c\lambda^{-1/2}\gamma\cdot\Gamma(\tfrac{1}{2})\cdot(t/\tau)^{1/2}. \tag{5}$$

$c$ is the dimensionless concentration,

$$c=\tfrac{4}{3}\pi R_0^3\rho. \tag{6}$$

This expression for $G^s(t)$ is appropriate for describing nondispersive transfer among randomly distributed chromophores. This limit is reached when there is insignificant inhomogeneous broadening (very large homogeneous linewidth) or when spectral diffusion occurs on a time scale that is much faster than the time for excitation hopping. In

both cases dynamic line broadening is much larger than the inhomogeneous linewidth.

### C. Dispersive excitation transfer

The dispersive transport theory, described in detail in Ref. 32, separates the calculation of EET dynamics into two parts. First, the extent to which the EET dynamics is dispersive is determined for the system for a given set of conditions: the dynamic linewidth, the inhomogeneous linewidth, $R_0$, $c$, and the excitation wavelength. This involves calculating, from the spectral overlap of dynamic line shapes, the effective concentration of acceptor chromophores and a scaling factor between the two limiting cases of the transfer. These results from the first part of the calculation are then applied to the expression describing nondispersive excitation transfer among a given spatial distribution of chromophores [Eq. (3)]. Since chromophores at a distribution of transition energies have some probability of being initially excited, the calculation is reiterated for excited chromophores at all possible transition energies in the inhomogeneous distribution, and the weighted average is taken as the observable.

For transfer among chromophores in a polymer glass, the dynamic and inhomogeneous linewidths were assumed to be time independent. The dispersive transport parameters did not change with time; in this case the time dependence to the transfer arose from the spatial distribution of acceptor chromophores.

To properly model dispersive transport in a liquid solution this calculation must be modified. This is because the spectral linewidths, which affect the EET through the calculation of spectral overlap—and subsequently the effective concentration of acceptors and scaling parameter—are time dependent. Spectral diffusion causes the dynamic linewidth to grow in time, the inhomogeneous linewidth to decrease, and the centers of the individual isochromats to shift toward the center of the inhomogeneous line. The effect of spectral diffusion on EET is through the time dependence of linewidths and line positions.

In the model of dispersive transfer, the spectral overlap of dynamic line shapes is identified with the probability that an excitation transfer step is DD. This step eliminates the need to consider the specifics of phonon emission and absorption in dispersive transfer. The spectral overlap, $F(\Delta E-\Delta E',t)$, of an excited chromophore with transition energy $\Delta E$ and an acceptor chromophore with energy $\Delta E'$ was calculated for all $\Delta E'$,

$$F(\Delta E-\Delta E',t) = \frac{\int_{-\infty}^{\infty} L_{\Delta E}(\omega,t)\cdot L_{\Delta E'}(\omega+(\Delta E-\Delta E'),t)d\omega}{\int_{-\infty}^{\infty} L(\omega,t)\cdot L(\omega,t)d\omega}. \quad (7)$$

$L_{\Delta E}(\omega,t)$ is the dynamic line shape centered at energy $\Delta E$. We have introduced time dependence to the spectral overlap through the time-evolving dynamic line shape. The denominator in Eq. (7) normalizes the probability to $F(\Delta E-\Delta E',t)=1$ when $\Delta E=\Delta E'$. $F(\Delta E-\Delta E',t)=1$ is the limit of donor–donor transfer, when the rate of back transfer is the same as the rate of forward transfer. If the initial transfer is to lower energy, Eq. (7) gives the probability that back transfer can occur (the transfer step is DD) aside from the spatial dependence. The DT limit is obtained when the quantity $F(\Delta E-\Delta E',t)=0$. Forward transfer to a lower-energy chromophore with phonon emission can take place, but back transfer cannot occur. If the initial transfer step is to an acceptor with higher energy, Eq. (7) gives the probability that the transfer occurs (aside from the spatial dependence).

The fraction of acceptor chromophores with transition energies lower than the energy of the initially excited chromophore ($\Delta E$) that participate in DD transfer is given by

$$d_r(\Delta E,t) = \frac{\int_0^{\Delta E} I(\Delta E',t)\cdot F(\Delta E-\Delta E',t)d(\Delta E')}{\int_0^{\Delta E} I(\Delta E',t)d(\Delta E',t)}. \quad (8)$$

$I(\Delta E',t)$ is the time-dependent inhomogeneous line shape. A similar expression, but with integration limits of $\Delta E$ to $\infty$ gives the donor fraction to the blue of a chromophore at $\Delta E$, $d_b(\Delta E,t)$.

The actual number density, $\rho$, of chromophores in a sample is measured spectroscopically. The number density to the red of $\Delta E$, $\rho_r$, and to the blue of $\Delta E$, $\rho_b$, are calculated by integrating the inhomogeneous line shape over appropriate limits, as done for the DD fraction,

$$\rho_r(\Delta E,t)=\rho\cdot\int_0^{\Delta E} I(\Delta E',t)d(\Delta E'),$$
$$\rho_b(\Delta E,t)=\rho\cdot\int_{\Delta E}^{\infty} I(\Delta E',t)d(\Delta E'). \quad (9)$$

Combining the equations for the donor fractions and the number densities leads to expressions for the number density of chromophores that can act as donors for an excited chromophore of transition energy $\Delta E$, $D(\Delta E,t)$, and the number density of traps, $T(\Delta E,t)$, chromophores that can accept an excitation but cannot back transfer to the originally excited chromophore,

$$D(\Delta E,t)=d_r(\Delta E,t)\rho_r(\Delta E,t)+d_b(\Delta E,t)\rho_b(\Delta E,t),$$
$$T(\Delta E,t)=\rho_r(\Delta E,t)\cdot[1-d_r(\Delta E,t)]. \quad (10)$$

$D(\Delta E,t)$ and $T(\Delta E,t)$ do not add up to $\rho$, the total number density. This is because there are chromophores of energy $\Delta E'$, to the blue of $\Delta E$, that have a low probability of accepting an excitation transfer from the initially excited chromophore because of the poor spectral overlap $F(\Delta E-\Delta E',t)$ for this energy separation. In this model, these are chromophores that are inaccessible for EET from the original chromophore because the phonons necessary to transfer the excitation up in energy are not available at the experimental temperature.

The calculation to this point has divided the distribution of acceptor chromophores into three groups depending on their electronic transition energies. $D(\Delta E,t)$ is the number density of chromophores which undergo DD

transport with the initially excited chromophore. $T(\Delta E,t)$ is the number density of chromophores which can only accept an excitation; they act as traps for the excited-state energy relative to the initially excited chromophore. And, finally there are chromophores to the blue of $\Delta E$ which cannot, or have a low probability of, accepting an excitation from the initially excited chromophore. The total number density of chromophores which can participate in energy transfer with a chromophore at $\Delta E$ is

$$\rho'(\Delta E,t)=D(\Delta E,t)+T(\Delta E,t). \tag{11}$$

In the nondispersive expression for $G^s(t)$ [Eq. (5)], the DD and DT cases differ only by a factor, $\lambda$. $\lambda$ has the limit of 1 for donor–trap and 2 for donor–donor transfer. With use of the procedure outlined above, the dispersive transport problem has been reduced to a problem of transfer in a mixture of donors and traps. It has been shown previously that scaling $\lambda$ linearly between the limits of $\lambda=1$ (pure DT) and $\lambda=2$ (pure DD),

$$\lambda(\Delta E,t)=1+\frac{D(\Delta E,t)}{\rho'(\Delta E,t)}, \tag{12}$$

is a good approximation for describing nondispersive EET in a mixture of donors and traps.[32]

The dispersive transport problem with spectral diffusion has now been reduced to a calculation which can be handled using the cumulant expansion treatment. In practice, the calculation progressively determines the change in $G^s(t)$ over time intervals $\Delta t$. At each time point $t$, the dynamic and inhomogeneous linewidths are calculated with the gate function and initial inhomogeneous and homogeneous linewidths (Sec. II A). The inhomogeneous distribution of transition frequencies is divided into discrete intervals. For each interval (centered at $\Delta E$), the spectral overlap is calculated with all possible acceptor intervals ($\Delta E'$). From the spectral overlap, the effective concentration of acceptor chromophores and the dispersive transport parameter are calculated. Then using the value of $G^s(t-\Delta t)$, the change in $G^s$ between $t-\Delta t$ and $t$ is calculated for each energy interval (centered at $\Delta E$) using Eq. (5). The ensemble-averaged change of $G^s$ results from repeating the calculation for all intervals $\Delta E$, and calculating the average weighted by the probability that a chromophore at $\Delta E$ was actually excited by the laser pulse of energy $\omega_\epsilon$, $N_{\omega_\epsilon}$:

$$N_{\omega_\epsilon}(\Delta E)=\frac{L(\omega_\epsilon-\Delta E,t=0)\cdot I(\Delta E,t=0)}{\int_0^\infty L(\omega_\epsilon-\Delta E,t=0)\cdot I(\Delta E,t=0)d(\Delta E)}. \tag{13}$$

### D. Model calculations of dispersive transfer with spectral diffusion

To calculate the effect of spectral diffusion on dispersive EET we assume that both the inhomogeneous and dynamic line shapes are Lorentzians of the form

$$L(\omega,t)=L_0\cdot\frac{1}{\omega^2+(\Delta\omega_d(t)/2)^2}, \tag{14}$$

where the full width at half maximum (FWHM), $\Delta\omega_d$, is time dependent. This functional form for the line shapes proves computationally convenient because the convolution of two Lorentzians is also a Lorentzian with FWHM given by the sum of the widths of the two curves. However, inhomogeneous broadening caused by dipole–dipole interactions can result in a Lorentzian line shape[43] and the dynamically broadened line can be Lorentzian as well.[44] $\Delta\omega_d(t)$ is calculated for the dynamic contribution to the $S_0$–$S_1$ transition using the homogeneous linewidth [dynamic width at $t=0$, $\Delta\omega_d(t=0)$], the absorption linewidth [$\Delta\omega_d(t=\infty)$], and Eqs. (1) and (2). The inhomogeneous linewidth is then adjusted to reflect motional narrowing. The total width of the line, $\Delta\omega_T$, is the sum of the dynamic and inhomogeneous linewidths. The inhomogeneous width is given by the difference of the total linewidth and the dynamic width, $\Delta\omega_T=\Delta\omega_d(t)+\Delta\omega_i(t)$. As the dynamic width increases the inhomogeneous width shrinks, leaving the total width unchanged. To preserve the overall line shape, the broadening of the dynamic lines is accompanied by shifts of each of the dynamic lines toward the center of the total line ($\Delta E_0$).

Since femtosecond time-scale photon-echo experiments have been performed on systems of organic dye molecules dissolved in viscous solvents,[2(a)] which are very similar to those studied here, we will employ these results. The measured electronic dephasing times ($T_2$) at room temperature for nile blue and malachite green in ethylene glycol are $\sim$60 fs. This corresponds to a homogeneous linewidth of 175 $cm^{-1}$. We use this value for $\Delta\omega_d(t=0)$. As discussed below, theoretical work by Loring[45] and low-temperature measurements made in the course of this work suggest an appropriate inhomogeneous linewidth of 600 $cm^{-1}$.

Figure 2 shows examples of the calculations made using the expressions developed in Secs. II A, II B, and II C. The concentration of chromophores is $3\times10^{-3}M$, $R_0=58$ Å. The calculation is repeated for three different excitation wavelengths: one on the blue side of the absorption line (a), one near the peak of the line (b), and one on the red side of the absorption line (c). The figure shows examples of calculations of $G^s(t)$ for different values of the rate of solvent fluctuations, $R$, at the three different excitation wavelengths. All parameters in the calculation are held constant except $R$. As $R$ changes, the extent of dispersive transfer also changes (compare to Fig. 1). When $R$ is very fast ($R=10$), transfer is nondispersive because the $S_0$–$S_1$ line is dynamically broadened at all but the shortest times. A small amount of dispersive transfer can be observed when $R$ is similar to $\tau$ ($R=1$), and transport becomes more dispersive as $R$ decreases further. For $R=0.01$ or less, the rate of spectral diffusion is much slower than the time scale for EET. This corresponds to the situation we have previously investigated in detail,[32] in which the dynamic and inhomogeneous linewidths do not change during the excited-state lifetime. For the linewidths used in the calculations, the curves for $R=0.01$ display the maximum extent of dispersive transport. For $R=10$, there is no difference in $G^s(t)$ for three different excitation wavelengths. This is the result that is predicted by the Förster

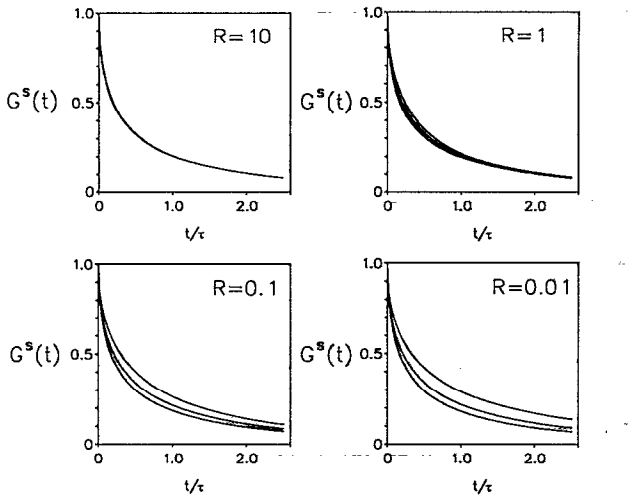


FIG. 2. Electronic excitation transfer calculated for various values of $R$, the rate of solvent fluctuations causing spectral diffusion. $R$ is parametrized in terms of excited-state lifetimes, $\tau$. Excitation wavelengths are 560, 570, and 580 nm. Parameters used for the calculations include $\Delta\omega_d(t=0) = 175\ \mathrm{cm}^{-1}$ (homogeneous linewidth), $\Delta\omega_i(t=0) = 600\ \mathrm{cm}^{-1}$ (inhomogeneous width at $t=0$), $c=1.5$ (Förster reduced concentration), $\Delta E_0 = 17\,300\ \mathrm{cm}^{-1}$ (optical line center). For $R=10$, $R$ is faster than the excitation transfer time scale (approximately $\tau$), excitation transfer is nondispersive. For $R=1$, the first signs of dispersive transport appear. As $R$ becomes slower than the time scale for EET, the transfer becomes more dispersive. For $R=0.01$, spectral diffusion is slow compared to EET; the maximum amount of dispersive transport is observed for the imput parameters.

theory for EET. However, Förster theory assumes the lines are homogeneously broadened. These calculations show that it is sufficient to have the fluctuation rate responsible for spectral diffusion a factor of 10 faster than the time scale for EET to reach the Förster limit.

This set of calculations demonstrates that the extent of dispersive transport can be directly related to the time scale for spectral diffusion. These model calculations also show that the rate of spectral diffusion can be investigated by observing the extent of dispersive transport.

## III. EXPERIMENTAL PROCEDURES

Solutions of rhodamine B perchlorate (Exciton) in glycerol (Baker) and in propylene glycol (Mallinckrodt) were prepared in an argon atmosphere. Rhodamine B (RB) is a weak acid and it was found that the absorption spectra were shifted slightly to the blue at low concentration ( $< 10^{-5}M$).[46] All solutions used in this study were acidified with a small amount of concentrated HCl, whereupon the absorption spectra for both the high- and low-concentration solutions were identical.

Aggregation of organic dye molecules has been reported at concentrations similar to those of the high-concentration samples used in this study.[47,48] RB is present predominantly as aggregates in water at $10^{-3}M$ concentration; it is considerably more soluble in ethanol.[49] For this reason, the solutions of RB in glycerol and propylene glycol were extensively checked for aggregation of the chromophores. Aggregates can be detected by a change in the shape of the absorption spectrum or shortening of the fluorescence lifetime due to excitation trapping at the aggregates.[47,48] Comparing the shapes of the absorption spectra for the high- and low-concentration solutions used in this study, the spectra are superimposable at all temperatures investigated. The fluorescence lifetime also gives no evidence of aggregates for concentrations up to $3 \times 10^{-3}M$. Upon increasing the dye concentration further, to $2 \times 10^{-2}M$, a distinctly different absorption spectrum was measured, and the fluorescence lifetime decreased dramatically, indicating aggregation at this concentration. All concentrations used in the measurements of excitation transport and solvent relaxation reported here were $3 \times 10^{-3}M$ or lower.

$3\times10^{-6}M$ solutions were used to measure the time-dependent orientational relaxation of the chromophore and the solvation dynamics of excited RB. These low-concentration samples were placed in 1 mm spectroscopic cuvettes; the optical density $\leqslant 0.1$. Intermolecular excited-state transfer was measured in higher-concentration solutions ( $\sim 10^{-3}M$). These solutions were sandwiched between two fused silica disks with 6 $\mu$m spacers to keep the optical densities low in spite of the high concentrations. This is important to avoid reabsorption of the fluorescence. Optical densities were between 0.1 and 0.2 at the peak of the absorption spectrum. Measurements at subambient temperatures were made by cooling high- and low-concentration samples in a given solvent simultaneously in a closed-cycle helium refrigerator.

Intermolecular electronic excitation transfer and reorientational motion of the excited chromophores were measured by time-resolved fluorescence depolarization. An anisotropic distribution of chromophores is excited by plane-polarized laser pulses tuned to a frequency in the $S_0$–$S_1$ absorption band. In low-concentration samples, reorientation of the emission transition dipole direction by molecular reorientation leads to a time-dependent decay of the anisotropy.[42,50,51] In high-concentration samples, excitation transfer from the initially excited RB chromophores (donors) to the isotropically oriented ensemble of unexcited RB molecules (acceptors) causes additional depolarization of the fluorescence.[5,8,52] From fluorescence decays detected with polarization parallel ($I_\parallel$) and perpendicular ($I_\perp$) to the excitation polarization direction, one obtains the fluorescence anisotropy $r(t)$,

$$r(t) = [I_\parallel(t) - I_\perp(t)]/[I_\parallel(t) + 2I_\perp(t)]. \tag{15}$$

The contribution to $r(t)$ from EET is $G^s(t)$,[5,11,12] the self-part of the Green-function solution to the master equation for excitation transfer. $G^s(t)$ is the probability that the initially excited chromophore remains excited after time $t$. $G^s(t)$ reflects excitations which have never left the initially excited chromophore, and excitations that have left and then returned. The reorientational contribution to the depolarization, $\Phi(t)$, is obtained from the anisotropy decay from low-concentration solutions. For relatively slow rotational motion, it is a good approximation to separate contributions from excitation transfer and reorientation, leading to

$$r(t)=C\cdot G^s(t)\cdot\Phi(t). \quad (16)$$

The constant $C$ accounts for the relative orientation of the absorption and emission transition dipole directions. $G^s(t)$ is obtained by dividing $r(t)$ for a high-concentration sample (EET occurs) by $r(t)$ for a low-concentration sample (no EET) under identical conditions, i.e., wavelength, temperature, etc. This divides out $C$ and $\Phi(t)$, yielding $G^s(t)$.

Fluorescence depolarization measurements were made by time-correlated single-photon counting. The apparatus[32] and technique[50] have been described in detail. The dye laser excitation pulses were tunable from 555 to 590 nm using rhodamine 575 as the gain medium. A detection system was employed that provided measurement of a broadband (~60 nm) of fluorescence around a tunable excitation wavelength. The center slit from a double 1/4 m, subtractive dispersive monochromator was replaced with a microscope slide attached to a translation stage. A narrow (~1 mm) black strip on the slide blocked the scattered laser light (over ~4 nm bandwidth), but fluorescence both to the blue and red of the excitation wavelength was passed. Upon changing excitation wavelengths, the grating angles were left unchanged, but the position of the strip on the slide was translated to block scattered light at the new excitation wavelength. The instrument response time was typically 60 ps, measured full width at half maximum.

Broadband detection around the laser excitation wavelength was used for two reasons. First, solvation of the excited chromophore by the polar solvent occurs on the same time scales as the fluorescence lifetime and intermolecular excitation transfer. Solvation leads to a time-dependent Stokes shift in the emission spectrum. The population decay from the $S_1$ excited state is complicated and nonexponential if detection is made over a narrow spectral region of the fluorescence.[53,54] Broadband detection of fluorescence from the excited chromophores allowed us to remove this as a possible source of depolarization. Second, the $S_0$–$S_1$ transition of rhodamine B contains a large degree of overlap between the absorption and emission spectra. In order to collect a large portion of the emission spectrum it was necessary to detect fluorescence both to the blue and red of the excitation wavelength, while excluding scattered laser light.

Time-resolved fluorescence spectra were also obtained using single-photon counting. Fluorescence was detected through a polarizer set at the magic angle with respect to the excitation polarization direction, to remove depolarization effects, and through a 1 m monochromator with slit widths set for a resolution of 2 Å. The fluorescence intensity in a predetermined time interval of the fluorescence decay, set by upper- and lower-level discriminators on the multichannel analyzer, was detected while the monochromator was scanned over the spectrum under computer control. A shutter was closed when the monochromator passed through the excitation wavelength to protect the phototube from scattered laser light. The time-resolved spectral measurements were not corrected for the instrument response (~100 ps with this monochromator) or for the spectral response of the monochromator grating or microchannel plate photomultiplier used to detect the fluorescence.

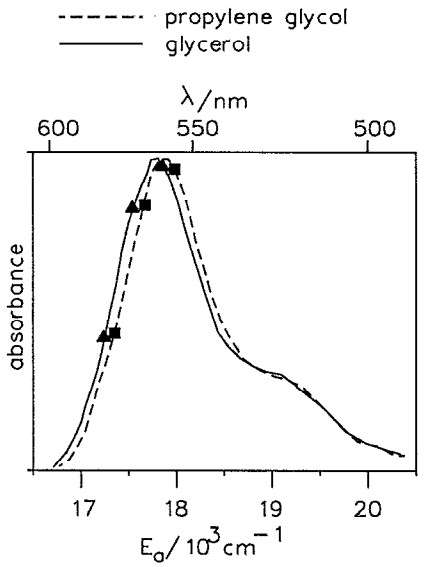


FIG. 3. $S_0$–$S_1$ electronic absorption of rhodamine B in glycerol (—) and propylene glycol (---) at room temperature. Excitation wavelengths used in this study are highlighted (▲, glycerol: 560, 570, 580 nm; ■, propylene glycol: 556, 566, 576 nm). Since the absorption spectrum in propylene glycol is shifted by ~4 nm to the blue relative to glycerol, the excitation wavelengths are adjusted to be the same relative to the peak in each solvent.

## IV. EXPERIMENTAL RESULTS

### A. Electronic excitation transfer

The $S_0$–$S_1$ electronic absorption spectra of RB in glycerol and in propylene glycol at room temperature are shown in Fig. 3. Excitation wavelengths used for the measurements reported here are indicated in the figure. The spectrum in propylene glycol is shifted 4 nm to the blue relative to glycerol; excitation wavelengths were chosen to be at the same relative position in the two spectra.

$G^s(t)$ curves for the $2.5\times10^{-3}M$ solution of rhodamine B in propylene glycol are shown in Fig. 4. The curves were obtained using Eq. (16) and the procedure described immediately below it. The decay of $G^s(t)$ is indicative of the rate and extent of EET. The figure shows the results obtained at three different temperatures, room temperature (297 K), 273 K, and 250 K. At each temperature, $G^s(t)$ is measured with different excitation wavelengths in the $S_0$–$S_1$ absorption band. At $T=297$ K, excitation at 556 nm, near the peak of the absorption spectrum (Fig. 3), leads to identical excited-state transfer dynamics as excitation at 576 nm, near the red edge of the absorption spectrum. This is the result predicted by the Förster theory for electronic excitation transfer (no dispersive transfer). $G^s(t)$ is not sensitive to the excitation wavelength. In propylene glycol at room temperature the $S_0$–$S_1$ electronic transition is completely dynamically broadened on the time scale of electronic excitation transfer (hundreds of picosec-

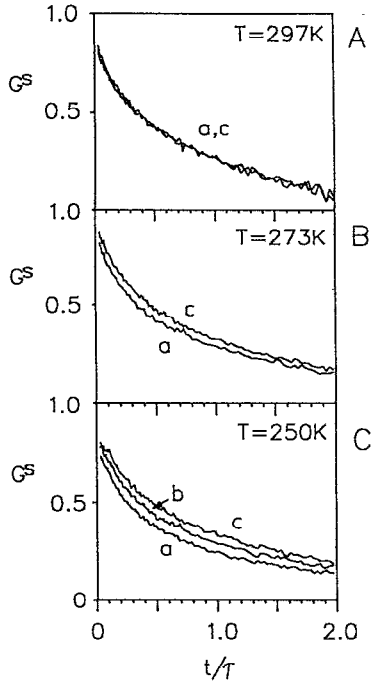


FIG. 4. $G^s(t)$ measured for $2.5 \times 10^{-3}M$ solution of rhodamine B in propylene glycol at different wavelengths and temperatures. The fluorescence lifetime $\tau$ is 3.3 ns in these solvents. (A) $T=297$ K, excitation at (a) 556 nm and (c) 576 nm. Excitation transfer is nondispersive at room temperature in propylene glycol. This is the result predicted by Förster theory. (B) $T=273$ K, excitation at (a) 556 nm and (c) 576 nm. At a temperature $\sim 100$ K above $T_g$ EET is dispersive in propylene glycol, demonstrating inhomogeneous spectral broadening that persists for the nanosecond time scale. (C) $T=250$ K, excitation at (a) 556 nm, (b) 566 nm, and (c) 576 nm. As the temperature decreases the amount of dispersive EET increases.

onds to nanoseconds). Spectral diffusion enables a chromophore to sample the entire line rapidly compared to the rate of excitation transfer. Photon-echo experiments[2(a)] on virtually identical systems demonstrate that it is spectral diffusion rather than homogeneous broadening that is responsible for the lack of dispersive transport at room temperature, since the echo-measured homogeneous linewidth is only approximately one-quarter of the total linewidth (see below).

When the temperature is lowered to 273 K, Fig. 4(b), a difference is observed in the decay of $G^s(t)$ for excitation at 556 and 576 nm. EET is dispersive in propylene glycol at this temperature, which is $\sim 100$ K above $T_g$ (Table I). Previous observations of dispersive energy transport at high temperatures, measured by fluorescence depolarization, were made on polymer systems below their glass transition temperatures.[32] Figure 4(b) demonstrates that dispersive EET can occur in liquids near room temperature. Observation of dispersive EET demonstrates that there is significant inhomogeneity in the optical transition on the timescale of excitation transfer.

At 250 K [Fig. 4(c)], there is an even greater amount of dispersive transfer. The relative contributions of dynamic and inhomogeneous broadening affect the extent of dispersive EET,[32] as shown in Fig. 2. The data reveal that

TABLE I. Properties of glycerol and propylene glycol.

| | | Propylene glycol | Glycerol |
|---|---|---|---|
| $T_g$ (K)[a] | | 172 | 193 |
| $\eta$ (cP):[b] | 297 K | 40 | 850 |
| | 273 K | 243 | 9000 |
| | 250 K | 2600 | $2.5\times10^5$ |

[a]Reference 59.
[b]Propylene glycol, Ref. 57(a); glycerol, Ref. 57(b).

the extent of inhomogeneous broadening that exists on the time scale of the observable, has increased significantly as the temperature is reduced from room temperature to 250 K.

Dispersive transport was also observed in solutions of RB in glycerol. The glass transition temperature is higher in glycerol than propylene glycol, and glycerol is more viscous at a given temperature (Table I). Dispersive EET is observed in glycerol even at room temperature. This is shown in Fig. 5(a) for a $3 \times 10^{-3}M$ solution. In Fig. 5(b) we see that there is a larger effect of the excitation wavelength on the EET at 250 K. Similar results have been obtained for a $1.5 \times 10^{-3}M$ solution of rhodamine B in glycerol. In the less-concentrated sample $G^s(t)$ decays less due to a lower density of acceptors, but the onset and extent of dispersive transfer is independent of the concentration.

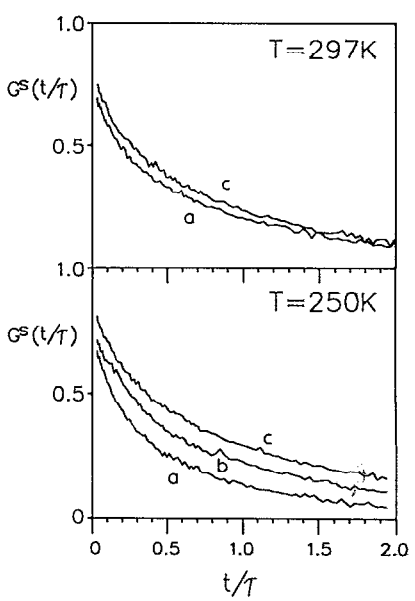


FIG. 5. $G^s(t)$ measured for a $3 \times 10^{-3}M$ solution of rhodamine B in glycerol. (A) $T=297$ K, excitation at (a) 560 nm and (c) 580 nm. Electronic excitation transfer is dispersive in glycerol at room temperature. (B) $T=250$ K. Glycerol is a supercooled liquid at this temperature and exhibits significant inhomogeneous broadening. This is reflected in a large amount of dispersive EET. Excitation is at (a) 560 nm, (b) 570 nm, and (c) 580 nm.

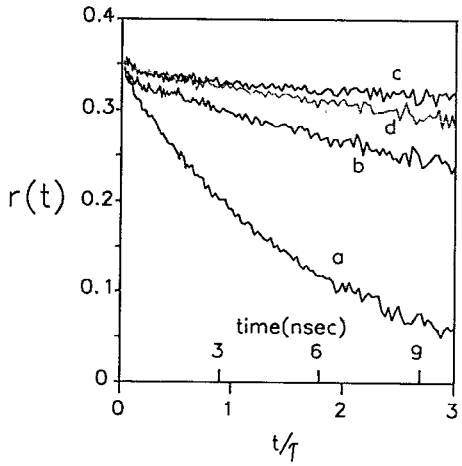


FIG. 6. Orientational relaxation of rhodamine B in propylene glycol at (a) $T=297$ K, (b) $T=273$ K, and (c) $T=250$ K, and in glycerol at $T=297$ K (d). The solution concentrations are $< 10^{-5}M$; the fluorescence anisotropy decays due to reorientation of the electronically excited probe (no excitation transport takes place). At room temperature rhodamine B reorients more slowly in the more viscous solvent, glycerol, in agreement with hydrodynamic theory. As the temperature is reduced, the mobility of the solvent molecules is reduced and the reorientation slows accordingly.

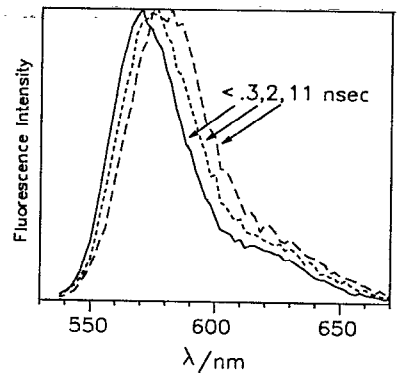


FIG. 7. Time-resolved emission spectra for a low-concentration solution ($< 10^{-5}M$) of rhodamine B in propylene glycol at $T=250$ K. No electronic excitation transfer takes place at this concentration. The fluorescence spectrum shifts to lower energy at longer times due to solvation of the excited probe molecule. The spectra are shown at $<0.3$, 2, and 11 ns after excitation.

Comparing results from glycerol and propylene glycol at 250 K and above, transport is more dispersive in glycerol. At the same temperature, RB electronic spectra in propylene glycol and glycerol have different contributions from dynamic and inhomogeneous spectral broadening on the experimental time scale. This is correlated with the viscosity of the liquids (Table I). At 200 K, near the glass transition temperatures, both liquids are extremely viscous and the transfer appears equally dispersive in the two solvents. The chromophore linewidth has similar contributions from inhomogeneous and dynamical line broadening in both solvents at this temperature.

### B. Reorientational dynamics

Reorientational dynamics and solvation dynamics in solutions of rhodamine B in propylene glycol and glycerol have been measured in order to compare the onset and extent of dispersive transfer to other molecular-scale dynamic properties. Figure 6 shows the fluorescence anisotropy decay for a low concentration ($3 \times 10^{-6}M$) RB/propylene glycol solution at (a) room temperature (297 K), (b) 273 K, and (c) 250 K, and for a $3 \times 10^{-6}M$ solution of RB in glycerol at room temperature (d). The concentration is too low for EET to occur [$G^s(t) = 1$]. The fluorescence anisotropy decays in time because of reorientational motion of excited RB molecules [$\Phi(t)$ in Eq. (16)]. This occurs on the several nanosecond time scale at room temperature in propylene glycol and on longer time scales as the temperature decreases. The probe molecule is essentially static with respect to reorientation on the time scale of the fluorescence lifetime (3.3 ns) at 250 K in propylene glycol and at room temperature in glycerol. At a given temperature the reorientation of the excited chromophore is faster in propylene glycol than in glycerol. This result is in agreement with hydrodynamic theory; the reorientation time is proportional to the viscosity divided by the temperature.[51]

### C. Solvation dynamics

The fluorescence spectra of low-concentration RB in glycerol and propylene glycol were measured at a series of times after excitation using time-correlated single-photon counting. Fluorescence spectra of a solution of RB in propylene glycol ($3 \times 10^{-6}M$) are shown in Fig. 7. The excitation wavelength is 556 nm; the sample temperature is 250 K. The peak heights have been normalized. The concentration of this solution is too low for EET to occur. Solvent relaxation causes the emission spectrum to shift to lower energy on the nanosecond time scale. Solvation of excited chromophores has been extensively studied for a number of dye molecules in solvents of varying characteristics.[53,54] The dipole moment of a RB molecule changes direction and magnitude upon electronic excitation. As the polar solvent reorganizes about the modified RB dipole, the energy difference between the initial Franck–Condon excited electronic state and the ground state is reduced. The solvation process has a complicated time dependence that depends on the dynamics of the solvent molecules and specific interactions between solvent and solute.

Figure 8 compares the rates of solvent relaxation for the same low-concentration rhodamine B/propylene glycol solution at three different temperatures, 273, 250, and 200 K. Excitation occurred at 556 nm, near the peak of the absorption spectrum. The peak of the emission spectrum is plotted vs time after excitation. At room temperature (not shown), the fluorescence spectrum completely relaxes in less than 1 ns after excitation. As the temperature is lowered, the Stokes shift becomes progressively slower. Similar measurements have been made for solutions of rhodamine B in glycerol. At a given temperature, the solvation dynamics occur more rapidly in propylene glycol than in glycerol, e.g., essentially no solvent relaxation occurs at

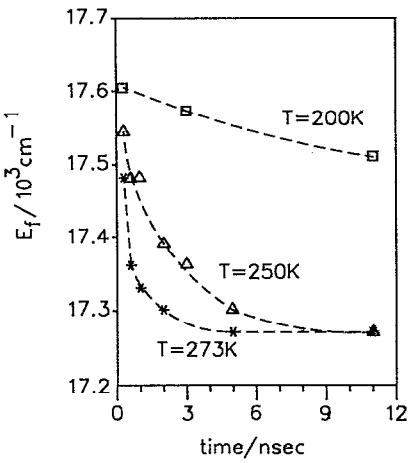


FIG. 8. Peak energy of the fluorescence spectrum (in $cm^{-1}$) plotted vs time after excitation for the low-concentration ($3 \times 10^{-6} M$) rhodamine B/propylene glycol solution. Excitation was at 556 nm. Temperatures shown are (*) 273 K, (△) 250 K, and (□) 200 K. As the temperature is lowered and solvent mobility reduced, solvent relaxation occurs more slowly.

250 K in glycerol. This is consistent with glycerol's greater viscosity at any temperature.

## V. COMPARISON OF THEORY AND DATA

In this section we compare the results of calculations made using the model developed in Sec. II to the measurements of dispersive EET in glycerol and propylene glycol that are presented in Sec. IV. The comparison permits a more quantitative consideration of the rate of spectral diffusion and a determination of the mechanism responsible for spectral diffusion.

Loring has recently developed a relationship between the inhomogeneous line shape of a chromophore and the thermodynamic free energy for the solute/solvent system, which is calculated from linearized solvation theories.[45] Monte Carlo simulations of line shapes for a dipolar hard-sphere solute in a dipolar hard-sphere solvent have also been performed. The results show that there is substantial inhomogeneous line broadening (hundreds of wave numbers) for a polar solute in a polar solvent. This arises from the orientation dependence of the dipole–dipole interaction between a chromophore and solvent molecules. We have measured the width of the lowest vibronic transition of $S_0$–$S_1$ for rhodamine B in glycerol at 90 K to be $\sim 600$ $cm^{-1}$. At this temperature the absorption spectrum is predominantly inhomogeneously broadened. These two results show that in systems such as rhodamine B in glycerol or propylene glycol, there is inhomogeneous broadening of hundreds of $cm^{-1}$ due to solute–solvent dipolar interactions.

Since dipole–dipole interactions between the solute and solvent cause extensive inhomogeneous broadening, it is clear that the time scale for the evolution of these interactions can determine the extent to which inhomogeneous broadening will be manifested in an EET experiment. In the limit that reorientation of the chromophores or the solvent dipoles occurs very quickly (relative to the time scale of EET) there will be no dispersive transport. The variations in the interaction energy between solvent and solute chromophore would be motionally averaged. If reorientation of dipoles occurs on the same time scale as the excitation transfer, the inhomogeneous broadening will continuously decrease throughout the experiment, while the dynamic linewidth increases due to spectral diffusion (Figs. 1 and 2).

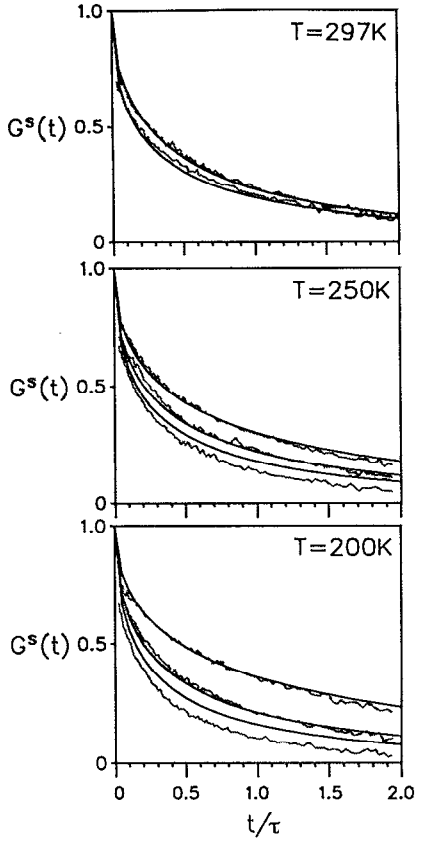


FIG. 9. Comparison of measurements of dispersive EET made on RB in glycerol ($3 \times 10^{-3} M$) with calculations of dispersive transfer made with the model described in Sec. II. The data are the same as shown in Fig. 5. The three excitation wavelengths are (from bottom to top) 560, 570, and 580 nm. At 297 K only 560 and 580 nm are shown. Parameters used for the calculations are $\Delta\omega_i(t=0) = 600\ cm^{-1}$, $\Delta E_0 = 17\,300\ cm^{-1}$, $c=1.5$. The homogeneous widths at each temperature are $T=297$ K, $\Delta\omega_d(t=0) = 175\ cm^{-1}$; $T=250$ K, $\Delta\omega_d(t=0) = 148\ cm^{-1}$; $T=200$ K, $\Delta\omega_d(t=0) = 50\ cm^{-1}$. The best-fit values of $R$, the fluctuation rate causing spectral diffusion, are given in Table II.

Figure 9 shows a comparison of calculations of dispersive transfer in glycerol to the experimental measurements of EET. The concentration of RB in glycerol is $3 \times 10^{-3} M$ (reduced concentration, $c=1.5$). The excitation wavelengths are the same as in Fig. 5: 560, 570, and 580 nm. For the calculations we have used the same parameters as for Fig. 2. $\Delta E_0 = 17\,300\ cm^{-1}$ and $\Delta\omega_i(t=0) = 600$ $cm^{-1}$. At room temperature the homogeneous linewidth is taken to be $\Delta\omega_d(t=0) = 175\ cm^{-1}$, the homogeneous linewidth observed by photon echoes for similar dye molecules in ethylene glycol.[2(a)] The homogeneous width is

TABLE II. Results of comparisons between data and fits to the dispersive transport model. $R$ is parametrized in terms of excited-state lifetimes (3.3 ns for RB in these solvents).

| Temperature (K) | $R\ (t/\tau)^{-1}$ Propylene glycol | Glycerol |
|---|---|---|
| 297 | 10 | 0.5 |
| 273 | 1 | ... |
| 250 | 0.1 | 0.01 |
| 200 | <0.01 | <0.01 |

unknown at the lower temperatures; it is scaled linearly down to 250 K (148 $cm^{-1}$) and set equal to 50 $cm^{-1}$ at 200 K. The adjustable parameter used in fitting the data is $R$, the fluctuation rate leading to spectral diffusion. $R$ is parametrized in terms of the excited-state lifetime, which is 3.3 ns for RB in these solvents. The values obtained from the comparison shown in Fig. 9 are given in Table II.

Considering the complexity of the problem, the calculations are in good agreement with the data. We believe the deviation observed for the excitation wavelength to the blue side of the $S_0$–$S_1$ transition (560 nm) arises from excitation into higher vibronic transitions of $S_0$–$S_1$. The fits are only sensitive to variations in $R$ when the dynamic linewidth is changing appreciably on the time scale of EET (approximately the excited-state lifetime, $\tau$). Therefore, for $R \ll 1/\tau$ the fit is insensitive to the value of $R$ (see Fig. 2).

Figure 10 shows a similar comparison made for a $2.5 \times 10^{-3}$ $M$ solution of RB in propylene glycol ($c=1.2$). Excitation wavelengths are 4 nm to the blue for RB in propylene glycol: 556, 566, and 576 nm, and $\Delta E_0$ = 17 420 $cm^{-1}$. The inhomogeneous linewidth at $t=0$ and homogeneous linewidths that are used in the calculations are identical to those used for glycerol. $R$ is varied to fit the data; the results of the fits are also given in Table II. Once again the data and calculations are in good agreement. At room temperature EET is nondispersive in propylene glycol (Fig. 4). Figure 2 demonstrates that $R \gtrsim 10$ at room temperature.

The results in Table II show that the rate of spectral diffusion is faster in propylene glycol than in glycerol. Below 250 K, where the rate of spectral diffusion becomes much slower than the rate of EET, the dispersive transport experiment cannot provide information on $R$ or distinguish a difference in the rates in glycerol and propylene glycol.

We can now compare the time scale for spectral diffusion measured by the dispersive EET measurement to the time scale for other molecular dynamics occurring in propylene glycol and glycerol. These include reorientation of the RB molecule, solvent relaxation, and reorientation of solvent molecules. In general, as the temperature decreases the rates of all the dynamical processes in glycerol and propylene glycol decrease. The viscosity increases (Table I), probe reorientation (Fig. 6) slows down, the time scale for solvent relaxation (Fig. 8) becomes longer, and the rate of spectral diffusion decreases (Table II).

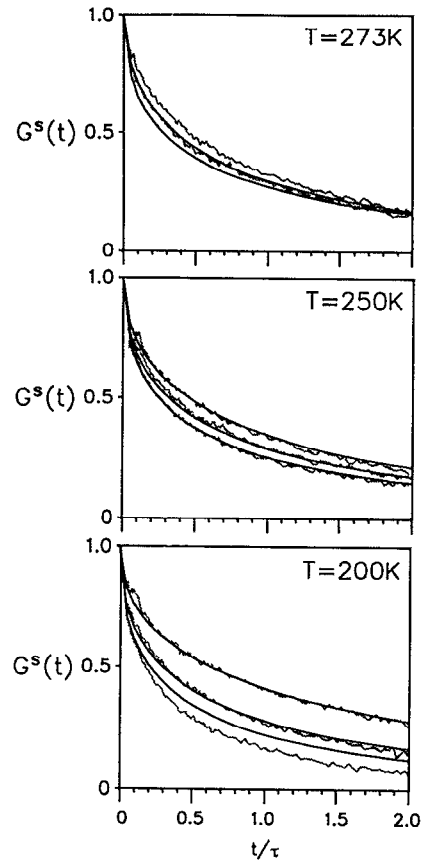


FIG. 10. Comparison of measurements of dispersive EET made on RB in propylene glycol ($2.5 \times 10^{-3} M$) with calculations of dispersive transfer made with the model described in Sec. II. The data are the same as shown in Fig. 4. The three excitation wavelengths are (from bottom to top in each figure) 556, 566, and 576 nm. Only 556 and 576 nm are shown at 273 K. Parameters used for the calculations are $\Delta\omega_i(t=0) = 600$ $cm^{-1}$, $\Delta E_0 = 17\,420$ $cm^{-1}$, $c=1.2$. The homogeneous widths at each temperature are $T=273$ K, $\Delta\omega_d(t=0) = 160$ $cm^{-1}$; $T=250$ K, $\Delta\omega_d(t=0) = 148$ $cm^{-1}$; $T=200$ K, $\Delta\omega_d(t=0) = 50$ $cm^{-1}$. The best-fit values of $R$, the fluctuation rate causing spectral diffusion, are given in Table II.

If the inhomogeneity is caused by the variations of the solvent dipolar fields at the various chromophores, reorientation of the chromophores will result in spectral diffusion. As a chromophore rotates, the interactions of its ground and excited states' dipole moments with the solvent field will change, and therefore the transition energy will change. The reorientational diffusion data shows that this is not the mechanism responsible for the spectral diffusion; the rate of reorientation of RB is too slow. At room temperature in propylene glycol no dispersive transport is observed. However, the reorientation correlation time is longer than one excited-state lifetime. Figure 2 shows that for $R=1$ (rate of spectral diffusion equal to the rate of excited-state decay), some dispersive transport should be observed. At 273 K, the reorientation is very slow. If chromophore reorientation is the mechanism responsible for spectral diffusion, the spectral line should be extensively inhomogeneously broadened on the time scale of EET, and EET should be highly dispersive. Nevertheless, Fig. 5

shows that EET is only mildly dispersive. The reorientation time for RB in glycerol is extremely slow at room temperature (curve d in Fig. 6), yet the EET is only slightly dispersive.

Comparing the results in Table II to the time scale for solvation (Fig. 8), we see that the fluctuations causing spectral diffusion occur more slowly than solvent relaxation. If $\tau_r$ is defined as the chromophore reorientation time, $\tau_s$ the solvation time, and $\tau_R$ the correlation decay time of the fluctuations leading to spectral diffusion, based on the data presented here: $\tau_r > \tau_R > \tau_s$. This relation applies to both propylene glycol and glycerol.

As we have discussed above, there is substantial evidence that the inhomogeneous broadening of the $S_0$–$S_1$ RB transition in propylene glycol and glycerol arises from dipolar interactions between solute and solvent.[45] As long as the solvent dipoles remain fixed relative to the RB dipole, the position of the chromophore in the inhomogeneous line will remain fixed. Reorientation of either the solute or solvent causes the dipole–dipole interaction to change, resulting in spectral diffusion. Reorientation of RB occurs too slowly to account for the rate of spectral diffusion. Data from light scattering[55] and NMR (Ref. 56) measurements of glycerol and ethylene glycol give a time scale for rotation of the dipolar groups (the hydroxy groups) of these two molecules. Their reorientation rate is determined by the rate that hydrogen bonds are broken. Dipolar segments in glycerol reorient in $\sim 1$ ns at room temperature; in ethylene glycol in $\sim 100$ ps.[55(b)] These times are not exactly the orientational relaxation times of the entire solvent molecules. However, they should be similar or slightly faster than the desired times. Ethylene glycol is almost equivalent to propylene glycol in that there are two hydroxy groups per molecule, and the viscosities differ by only a factor of 2 at room temperature.[57(a)] We have made estimates of the reorientation times at lower temperatures based on the changes in viscosity with temperature.

The time scales for solvent reorientation is the correct time scale to account for the observed spectral diffusion. Thus, we propose that orientational diffusion of solvent molecules causes fluctuations in the dipolar interactions between RB and the polar solvent that lead to spectral diffusion. Therefore, the rate of decay of the orientational correlation function becomes the rate of spectral diffusion. The probability of finding a chromophore in its initial location in the inhomogeneous line decays as the solvent orientational correlation-function decays. Here for simplicity we have taken the decay of the orientational correlation function to be a single exponential with decay rate, $R$. It is this rate that is used in the gate function to calculate the time dependence of spectral diffusion. The nature of the theory for spectral diffusion[19(b)] permits any form of the fluctuation rate distribution. Therefore it is possible to employ a distribution of rates. For our purposes here, a single rate is adequate.

The difference in the time scales for spectral diffusion and solvation probably arises from the range of solvent orientational motions that is required for each process. Spectral diffusion involves full loss of correlation of the solvent dipoles' orientations. Solvation is caused by small changes in the solvent dipoles' orientations restricted by the local solvent structure. Restricted orientational relaxation[58] occurs at a faster rate than full loss of orientational correlation responsible for spectral diffusion.

## VI. CONCLUDING REMARKS

Femtosecond photon-echo experiments in room-temperature viscous liquids measure the homogenous dephasing time and reveal that the optical-absorption spectrum is inhomogeneously broadened on the femtosecond time scale. They do not determine on what time scale the spectrum becomes dynamically broadened through spectral diffusion. The solute chromophore experiences a wide variety of solvent configurations that modify the solute's electronic structure. On the femtosecond time scale, these distinct solvent environments give rise to inhomogeneous broadening. On a sufficiently long time scale, all solvent configurations will be sampled by a chromophore. The measurement of the rate of spectral diffusion using EET demonstrates that the time scale for spectral diffusion for ionic dyes in viscous hydrogen-bonding solvents is orders of magnitude longer than the time scale for homogeneous dephasing. The femtosecond echo experiments show that the homogeneous linewidth is approximately one-quarter of the total linewidth. The rest of the linewidth is sampled on a nanosecond time scale by spectral diffusion.

Recent theoretical work by Walsh and Loring[1] has addressed the mechanism for femtosecond dephasing in liquids. Walsh and Loring make a convincing argument that the ultrafast dephasing arises from near-neighbor collisions between the chromophore and the solvent molecules. These collisions (position fluctuations) change the local chromophore–solvent potential, causing the energy fluctuations responsible for homogeneous dephasing. The collisions are caused by the ultrafast thermal fluctuations in local position of the solvent molecules. On a much longer time scale, these fluctuations lead to macroscopic diffusion. On the femtosecond time scale, the positions of molecules are essentially fixed. Displacement by diffusion is on the order of 0.01 Å compared to molecular sizes of several Å. On the ultrafast time scale, these fluctuations in position are more akin to the phonon-induced fluctuations in crystals. In contrast, the experiments presented here demonstrate that the nanosecond time scale spectral diffusion is caused by randomization of the local solvent structure by rotational diffusion (and possibly translational diffusion). A chromophore is excited in the presence of an electric dipolar field produced by the solvent. This field determines the position of the chromophore transition energy in the inhomogeneous line. As the orientational correlation function associated with the solvent molecules decays, the dipolar field also loses correlation with its $t=0$ value. As the dipolar field correlation function decays, the spectrum becomes dynamically broadened by spectral diffusion.

While spectral diffusion involves the randomization of dipole orientations, solvent relaxation involves correlated changes in dipole orientations. The local solvent structure

determines the dipolar field at the instant of optical excitation of the solute chromophore. Excitation changes the chromophore's dipole moment. The solvent structure evolves under the influence of the changed dipolar field produced by the chromophore. This is a relaxation of the local structure to a related structure rather than a randomization. While this relaxation involves changes in orientation and position of the solvent molecules, it occurs more rapidly than the total randomization that is responsible for spectral diffusion. The fact that the relaxed solvent structures are correlated with the original structures is demonstrated by the observation of the wavelength dependence of EET even when the system is undergoing fast solvent relaxation. EET occurs on a longer time scale than solvent relaxation in, for example, RB in propylene glycol at 273 or 250 K, yet these samples display a wavelength dependence. If solvent relaxation randomized the local solvent structures prior to EET, the wavelength dependence would not be observed.

The determination of the rate of spectral diffusion using the dispersive EET experiments permits a firm prediction to be made about the outcome of femtosecond stimulated echo experiments. In the model used here, there are only two time scales and two mechanisms that influence optical dephasing, the femtosecond time scale for solvent–chromophore collisions and the nanosecond time scale for the relaxation of the dipolar field at the chromophore by solvent orientational randomization. The femtoscale timescale dynamics result in homogeneous dephasing and the nanosecond dynamics give rise to spectral diffusion. The photon echo measures homogeneous dephasing. The stimulated echo measures a combination of homogeneous dephasing and spectral diffusion. The model and measurements presented here predict that as $T_w$ approaches the nanosecond time scale in RB in propylene glycol at 273 K or in glycerol at room temperature, the stimulated echo decay will become faster. The decay rate will increase approximately a factor of 4 as $T_w$ increases from a fraction of 1 ns to 10 ns. For times longer than 10 ns, the decay rate will no longer increase appreciably with increasing $T_w$. Because of the very fast decay times implied by these predictions, examining spectral diffusion in a system like this is a severe challenge to the femtosecond nonlinear spectroscopist. Therefore, other methods, like the one described here, are useful for the investigation of spectral diffusion in liquids.

## ACKNOWLEDGMENTS

We would like to thank Dr. Mark A. Dugan for useful conversations and to acknowledge the U.S. Department of Energy, Office of Basic Energy Sciences (Grant No. DE-FG03-84ER13251) for support of this research. Additional equipment support was provided by the NSF, Division of Materials Research (Grant No. DMR90-22675). We would also like to thank the Stanford Center for Materials Research Polymer Thrust Program for support of this research and for the use of the CMR picosecond fluorescence instrument.

[1] A. M. Walsh and R. F. Loring, Chem. Phys. Lett. **186**, 77 (1991); J. Chem. Phys. **94**, 7575 (1991).
[2] (a) P. C. Becker, H. L. Fragnito, J. Y. Bigot, C. H. Brito-Cruz, R. L. Fork, and C. V. Shank, Phys. Rev. Lett. **63**, 505 (1989); (b) E. T. J. Nibbering, D. A. Wiersma, and K. D. Duppen, *ibid.* **66**, 2464 (1991).
[3] *Molecular Dynamics in Restricted Geometries*, edited by J. Klafter and J. M. Drake (Wiley, New York, 1989).
[4] M. D. Ediger and M. D. Fayer, Int. Rev. Phys. Chem. **4**, 207 (1985).
[5] C. R. Gochanour and M. D. Fayer, J. Phys. Chem. **85**, 1989 (1981).
[6] C. R. Gochanour, H. C. Anderson, and M. D. Fayer, J. Chem. Phys. **68**, 1879 (1978).
[7] V. M. Agranovich and M. D. Galanin, *Electronic Excitation Transfer in Condensed Matter* (North-Holland, New York, 1982).
[8] F. W. Craver and R. S. Knox, Mol. Phys. **22**, 385 (1971).
[9] W. Y. Ching, D. L. Huber, and B. Barnett, Phys. Rev. B **17**, 5025 (1978); D. L. Huber, D. S. Hamilton, and B. Barnett, *ibid.* **16**, 4642 (1978).
[10] M. D. Ediger, R. P. Domingue, and M. D. Fayer, J. Chem. Phys. **80**, 1246 (1984); A. H. Marcus and M. D. Fayer, *ibid.* **94**, 5622 (1991).
[11] J. Baumann and M. D. Fayer, J. Chem. Phys. **85**, 4087 (1986).
[12] K. A. Peterson and M. D. Fayer, J. Chem. Phys. **85**, 4702 (1986).
[13] A. K. Roy and A. Blumen, J. Chem. Phys. **91**, 4353 (1989).
[14] I. Yamazaki, N. Tamai, and T. Yamazaki, J. Phys. Chem. **94**, 516 (1990).
[15] O. Pekcan, M. A. Winnik, and M. D. Croucher, Phys. Rev. Lett. **61**, 641 (1988).
[16] K. A. Peterson, A. D. Stein, and M. D. Fayer, Macromolecules **23**, 111 (1990).
[17] Th. Förster, Ann. Phys. (Leipzig) **2**, 55 (1948); Z. Naturforsch. A **4**, 321 (1949).
[18] G. Liu and J. E. Guillet, Macromolecules **23**, 1388 (1990); G. Liu, J. E. Guillet, E. T. B. Al-Takrity, A. D. Jenkins, and D. R. M. Walton, *ibid.* **23**, 1393 (1990).
[19] (a) L. R. Narasimhan, K. A. Littau, D. W. Pack, Y. S. Bai, A. Elschner, and M. D. Fayer, Chem. Rev. **90**, 439 (1990), and references therein; (b) Y. S. Bai and M. D. Fayer, Phys. Rev. B **39**, 11 066 (1989).
[20] K. A. Littau and M. D. Fayer, Chem. Phys. Lett. **176**, 551 (1991); K. A. Littau, M. A. Dugan, S. Chen, and M. D. Fayer, J. Chem. Phys. (to be published).
[21] *Dynamical Processes in Excited States of Solids*, edited by R. S. Metzler, J. E. Rives, and W. M. Yen (North-Holland, Amsterdam, 1990), also published as J. Lumin. **45** (1990).
[22] *Persistent Spectral Hole-Burning: Science and Applications*, edited by W. E. Moerner (Springer-Verlag, Berlin, 1988).
[23] I. Abella, N. A. Kurnit, and S. R. Hartmann, Phys. Rev. **141**, 391 (1966).
[24] C. A. Walsh, M. Berg, L. R. Narasimhan, and M. D. Fayer, Acc. Chem. Res. **20**, 120 (1987).
[25] R. M. Macfarlane and R. M. Shelby, J. Lumin. **36**, 179 (1987).
[26] (a) W. Breinl, J. Friedrich, and D. J. Haarer, J. Chem. Phys. **81**, 3915 (1984); (b) G. Schulte, W. Grond, D. Haarer, and R. J. Silbey, Chem. Phys. **88**, 679 (1988); (c) K. A. Littau, Y. S. Bai, and M. D. Fayer, J. Chem. Phys. **92**, 4145 (1990).
[27] C. H. Brito-Cruz, R. L. Fork, W. H. Knox, and C. V. Shank, Chem. Phys. Lett. **132**, 341 (1986).
[28] S. Kinoshita, H. Itoh, H. Murakami, H. Miyasaka, T. Okada, and N. Mataga, Chem. Phys. Lett. **166**, 123 (1990).
[29] T. J. Kang, J. Yu, and M. Berg, Chem. Phys. Lett. **174**, 476 (1990).
[30] S. Mukamel, Phys. Rev. A **28**, 3480 (1983); R. F. Loring, J. Y. Yan, and S. Mukamel, J. Chem. Phys. **87**, 5840 (1987).
[31] M. Berg, C. A. Walsh, L. R. Narasimhan, K. A. Littau, and M. D. Fayer, J. Chem. Phys. **88**, 1564 (1988).
[32] A. D. Stein, K. A. Peterson, and M. D. Fayer, Chem. Phys. Lett. **161**, 16 (1989); J. Chem. Phys. **92**, 5622 (1990).
[33] A. D. Stein and M. D. Fayer, Chem. Phys. Lett. **176**, 159 (1991).
[34] K. D. Rockwitz and H. Bässler, Chem. Phys. **70**, 307 (1982); R. Richert and H. Bässler, J. Chem. Phys. **84**, 3567 (1986).
[35] D. L. Huber and W. Y. Ching, Phys. Rev. B **18**, 5320 (1978).
[36] T. Holstein, S. K. Lyo, and R. Orbach, in *Topics in Applied Physics: Laser Spectroscopy of Solids, Vol. 49*, edited by W. M. Yen and P. M. Selzer (Springer-Verlag, Berlin, 1981).
[37] P. Avouris, A. Campion, and M. A. El-Sayed, *Advances in Laser Spectroscopy I, Vol. 113* (Society of Photo-Optical Instrumentation Engineers, Bellingham, WA, 1977).

[38] R. P. Parson and R. Kopelman, J. Chem. Phys. **82**, 3692 (1985).
[39] B. Movaghar, M. Grünewald, B. Ries, H. Bässler, and D. Würtz, Phys. Rev. B **33**, 5545 (1986); M. Grünewald, B. Pohlmann, B. Movaghar, and D. Würtz, Philos. Mag. B **49**, 341 (1984).
[40] S. K. Lyo, Phys. Rev. B **22**, 3616 (1980); G. Schönherr, H. Bässler, and M. Silver, Philos. Mag. B **44**, 47 (1981); R. Richert, B. Ries, and H. Bässler, *ibid.* **49**, L25 (1984).
[41] H. C. Meijers and D. A. Wiersma, Chem. Phys. Lett. **181**, 312 (1991).
[42] J. R. Lakowicz, *Principles of Fluorescence Spectroscopy* (Plenum, New York, 1982).
[43] J. R. Klauder and P. W. Anderson, Phys. Rev. **125**, 912 (1962); P. Hu and S. R. Hartmann, Phys. Rev. B **9**, 1 (1974); W. B. Mims, Phys. Rev **168**, 370 (1968).
[44] R. Kubo, in *Fluctuation, Relaxation, and Resonance in Magnetic Systems, Proceedings of the Scottish University's Summer School* edited by D. ter Haar (Oliver and Boyd, London, 1961); B. Di Bartolo, *Optical Interactions in Solids* (Wiley, New York, 1968).
[45] R. F. Loring, J. Phys. Chem. **94**, 513 (1990); N. E. Shemetulskis and R. F. Loring, J. Chem. Phys. **95**, 4756 (1991).
[46] J. Ferguson and A. W. H. Mau, Chem. Phys. Lett. **17**, 543 (1972); Aust. J. Chem. **26**, 1617 (1973); M. Faraggi, P. Peretz, I. Rosenthal, and D. Weinraub, Chem. Phys. Lett. **103**, 310 (1984).
[47] D. R. Lutz, K. A. Nelson, C. R. Gochanour, and M. D. Fayer, Chem. Phys. **58**, 325 (1981).
[48] P. R. Hammond, J. Chem. Phys. **70**, 3884 (1979).
[49] I. Lopez-Arbeloa and P. Ruiz Ojeda, Chem. Phys. Lett. **79**, 347 (1981); **87**, 556 (1982).
[50] D. V. O'Connor and D. Phillips, *Time-Correlated Single Photon Counting* (Academic, London, 1984).
[51] *Rotational Dynamics of Small and Macromolecules*, edited by Th. Dorfmuller and R. Pecora (Springer-Verlag, Berlin, 1987).
[52] M. D. Galanin, Tr. Fiz. Inst. im. P. N. Lebedeva Akad. Nauk SSSR **5**, 341 (1950).
[53] J. D. Simon, Acc. Chem. Res. **21**, 128 (1988), and references therein.
[54] P. F. Barbara and W. Jarzeba, Adv. Photochem. **15**, 1 (1990), and references therein.
[55] (a) H. Dux and T. Dorfmuller, Chem. Phys. **40**, 219 (1979); (b) D. A. Pinnow, S. J. Candau, and T. A. Litovitz, J. Chem. Phys. **49**, 347 (1968).
[56] L. J. Burnett and S. B. W. Roeder, J. Chem. Phys. **60**, 2420 (1974).
[57] (a) *Glycols*, edited by G. O. Curme and F. Johnston, ACS Monograph Ser. 114 (Reinhold, New York, 1952), p. 238; (b) R. Piccirelli and T. A. Litovitz, J. Acoust. Soc. Am. **29**, 1009 (1957).
[58] C. C. Wang and R. Pecora, J. Chem. Phys. **72**, 5333 (1980); J. K. Park, R. Pecora, and A. C. Ouano, Macromolecules **21**, 1722 (1988).
[59] N. O. Birge, Phys. Rev. B **34**, 1631 (1986); C. A. Angell and D. L. Smith, J. Phys. Chem. **86**, 3845 (1982).